The Astrophysical Journal Supplement Series, 268:6 (10pp), 2023 September https://doi.org/10.3847/1538-4365/ace444

General Physical Properties of Fermi Blazars

Yongyun Chen (陈永云)[1], Qiusheng Gu (顾秋生)[2], Junhui Fan (樊军辉)[3], Xiaoling Yu (俞效龄)[1], Xiaogu Zhong (钟晓谷)[1], Hongyu Liu (刘红宇)[1], Nan Ding (丁楠)[4], Dingrong Xiong (熊定荣)[5], and Xiaotong Guo (郭晓通)[6]
[1] College of Physics and Electronic Engineering, Qujing Normal University, Qujing 655011, People's Republic of China; ynkmcyy@yeah.net
[2] School of Astronomy and Space Science, Nanjing University, Nanjing 210093, People's Republic of China; qsgu@nju.edu.cn
[3] Center for Astrophysics, Guangzhou University, Guangzhou 510006, People's Republic of China
[4] School of Physical Science and Technology, Kunming University, 650214, People's Republic of China
[5] Yunnan Observatories, Chinese Academy of Sciences, Kunming 650011, People's Republic of China
[6] Anqing Normal University, 246133, People's Republic of China
Received 2023 April 4; revised 2023 June 6; accepted 2023 June 29; published 2023 August 22

Abstract

We study the general physical properties of Fermi blazars using the Fermi fourth source catalog data (4FGL-DR2). The quasi-simultaneous multiwavelength data of Fermi blazars are fitted by using the one-zone leptonic model to obtain some physical parameters, such as jet power, magnetic field, and Doppler factor. We study the distributions of the derived physical parameters as a function of black hole mass and accretion disk luminosity. The main results are as follows. (1) For a standard thin accretion disk, the jet kinetic power of most flat-spectrum radio quasars can be explained by the Blandford–Payne (BP) mechanism. However, the jet kinetic power of most BL Lacertae objects (BL Lacs) cannot be explained by either the Blandford–Znajek mechanism or the BP mechanism. The BL Lacs may have advection-dominated accretion flows surrounding their massive black holes. (2) After excluding the redshift, there is a moderately strong correlation between the jet kinetic power and jet radiation power and the accretion disk luminosity for Fermi blazars. These results confirm a close connection between jet and accretion. The jet kinetic power is slightly larger than the accretion disk luminosity for Fermi blazars. (3) There is a significant correlation between jet kinetic power and gamma-ray luminosity and radio luminosity for Fermi blazars, which suggests that gamma-ray luminosity and radio luminosity can be used to indicate the jet kinetic power.

Unified Astronomy Thesaurus concepts: Active galactic nuclei (16); Gamma-rays (637); Gamma-ray sources (633); BL Lacertae objects (158); Flat-spectrum radio quasars (2163); Jets (870)

Supporting material: machine-readable table

1. Introduction

Blazars are a special subclass of active galactic nuclei (AGNs), whose jet is directed at the observer (Urry & Padovani 1995). Blazars are usually divided into flat-spectrum radio quasars (FSRQs) and BL Lacertae objects (BL Lacs) according to the equivalent width (EW) of their optical emission lines. FSRQs have strong broad emission lines, and the EW of their emission lines is greater than 5 Å. BL Lacs show weak or no broad emission lines, and the EW of their emission lines is less than 5 Å. However, arbitrary classification based on EW is not enough. On one hand, Blandford & Rees (1978) suggested that the lack of broad emission lines in the BL Lacs may be due to the Doppler-boosted continuum swamping out any spectral lines. On the other hand, the detection of broad emission lines may be the result of the low jet-activity states (Vermeulen et al. 1995). Therefore, the physical difference between FSRQs and BL Lacs cannot be revealed by EW blazar classification mechanism. Some authors have proposed a more physical classification mechanism for blazars. Ghisellini et al. (2011) and Sbarrato et al. (2012) proposed that the broad-line region (BLR) luminosity ($L_{\rm BLR}$) in Eddington units can distinguish FSRQs from BL Lacs. The FSRQs have $L_{\rm BLR}/L_{\rm Edd} \geqslant 10^{-3}$ or $L_{\rm BLR}/L_{\rm Edd} \geqslant 5 \times 10^{-4}$, which, in turn, indicates a radiatively efficient accretion process ($L_{\rm disk}/L_{\rm Edd} \geqslant 0.01$). The BL Lacs have a radiatively inefficient accretion flow.

The formation of relativistic jets in AGNs has always been a hot issue in astrophysics, and their formation mechanism has not been clear. Many theoretical models have been proposed to explain the formation of the jets. Among the current theoretical models of jet formation, there are two main theories. One is the Blandford–Znajek (BZ) mechanism (Blandford & Znajek 1977), in which the jet extracts the rotational energy of the black hole. The other is the Blandford–Payne (BP) mechanism (Blandford & Payne 1982), where the jets mainly extract the rotational energy of the accretion disk. In both cases, the magnetic field plays a major role in directing power from a black hole or disk into the jet; in both cases, it should be maintained by matter accreted to the black hole, leading to an expected relationship between accretion and jet power (Maraschi & Tavecchio 2003). Chai et al. (2012) found a significant correlation between black hole mass and the bulk Lorentz factor using 101 radio-loud AGNs. They suggested that the BZ mechanism may dominate over the BP mechanism in these radio-loud AGNs. Zhang et al. (2022) proposed that the jets of both FSRQs and BL Lacs are likely produced by the BZ mechanism. Foschini (2011) compared the maximum jet power of the BZ mechanism with the observed jet power and suggested that the jets of FSRQs cannot be fully explained by the BZ mechanism. However, at present, it is not clear whether the BZ mechanism or the BP mechanism dominates the jet formation of the Fermi blazars.

Since the successful launch of the Fermi Space Telescope, many AGNs have been detected with high-energy gamma-ray radiation (Abdo et al. 2009, 2010a; Nolan et al. 2012; Acero et al. 2015; Abdollahi et al. 2020; Ajello et al. 2022), especially blazars, confirming that these AGNs have strong relativistic jets. Encouraged by the availability of high-quality multiwavelength (MW) data sets of large samples of Fermi blazars, we systematically study their broadband properties by using observational and theoretical spectral energy distribution (SED) modeling methods. Our main goal is to study the basic properties of Fermi blazars, such as the relationship between accretion and jets, and the formation mechanism of the jets. Compared with previous studies, we focus on the observed results and then use a leptonic emission model to explain them. Here, we show the results of our research on blazars included in the Fermi Large Area Telescope (LAT) fourth source catalog data release 2 (4FGL-DR2; Abdollahi et al. 2020). Our sample is probably the largest sample that applies the physical SED model. In Section 2, we describe the sample. Section 3 shows the model of jets. Section 4 describes the results and discussion. Section 5 is the conclusion.

2. The Sample

2.1. The Fermi Blazar Sample

Paliya et al. (2021) used the 4FGL-DR2 catalog to get the 1077 Fermi blazars with black hole mass and accretion disk luminosity. We carefully examined the sample of Paliya et al. (2021) and compared it with the source classification of Abdollahi et al. (2020) and Foschini et al. (2021). We only consider sources that have reliable redshift, black hole mass, accretion disk luminosity, 1.4 GHz radio flux, and quasi-simultaneous multiwavelength data. The redshift, black hole mass, and accretion disk luminosity come from the work of Paliya et al. (2021). The 1.4 GHz radio flux comes from the NASA/IPAC Extragalactic Database. The quasi-simultaneous multiwavelength data comes from the Space Science Data Center SED Builder.[7] We get 459 Fermi blazars (317 FSRQs, and 142 BL Lacs: 41 low-synchrotron-peaked BL Lacs (LBLs), 18 intermediate-synchrotron-peaked BL Lacs (IBLs), and 83 high-synchrotron-peaked BL Lacs (HBLs)). The boundaries of BL Lacs are $\log \nu_{\rm p} < 14$ Hz for LBLs, Hz $14 < \log \nu_{\rm p} < 15$ Hz for IBLs, and $\log \nu_{\rm p} > 15$ Hz for HBLs (e.g., Abdo et al. 2010b).

2.2. The Jet Power

The quasi-simultaneous multiwavelength data of Fermi blazars are modeled with a simple one-zone leptonic emission model (Tramacere et al. 2009, 2011; Tramacere 2020). The broadband SEDs have been modeled using the open-source package JetSet[8] numerical leptonic code (Tramacere 2020). According to the the minimum χ^2/degrees of freedom, the parameters were defined as the best-fit values (see Figure 1). We estimate the jet power of electrons ($P_{\rm ele}$), Poynting flux ($P_{\rm mag}$), radiation ($P_{\rm rad}$), and protons ($P_{\rm p}$) as follows:

$$P_i = \pi R^2 \Gamma^2 \beta c U_i^{'}, \tag{1}$$

where U_i' is the energy density of the i component, which is protons ($i = p$), relativistic electrons ($i = e$), the magnetic field

7 http://tools.ssdc.asi.it/SED/
8 https://jetset.readthedocs.io/en/latest/

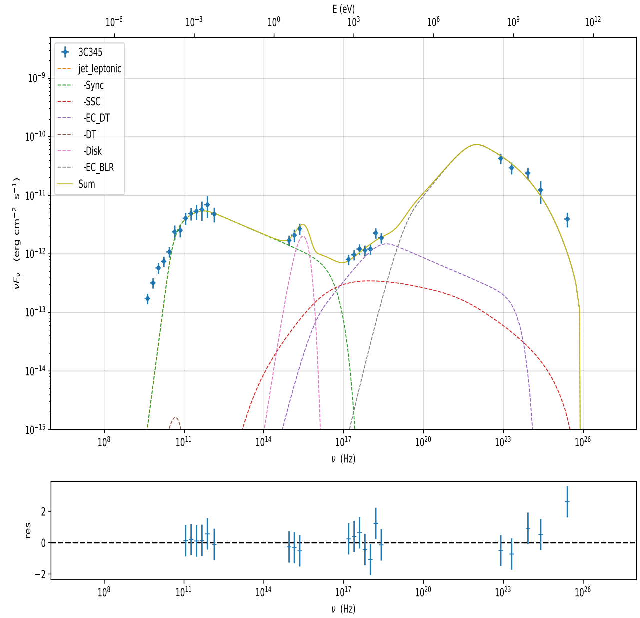

Figure 1. The example of broadband SEDs of 3C345 is modeled by using a one-zone model.

($i = B$) and the produced radiation ($i =$ rad). The radiative power is derived as

$$P_{\rm rad} = \pi R^2 \Gamma^2 \beta c U_{\rm rad}^{'}, \tag{2}$$

where $U_{\rm rad}'$ is the radiation energy density ($U_{\rm rad}' = L'/(4\pi R^2 c)$). L' is the total observed nonthermal luminosity in the comoving frame. δ is the Doppler factor, $\delta = (\Gamma(1 - \beta\cos\theta))^{-1}$, where θ is the angle between the jet axis and the line of sight of the observer. Γ is the Lorentz factor. For blazars, we have sin $(\theta) \approx 1/\Gamma$ and, thus, $\Gamma \simeq \delta$ (Ghisellini et al. 2014). β is the jet relativistic speed, $\beta = \sqrt{1 - 1/\Gamma^2}$. The size of the emission region can be derived from the relation $R = ct_{\rm var}\delta/(1 + z)$ (Ghisellini et al. 2014), where $t_{\rm var}$ is the variability timescale. The relevant data is shown in Table 1. The example is shown in Figure 1.

3. The Jet Model

Some authors have calculated the maximum jet power that can be extracted from a rapidly rotating black hole/magnetized accretion disk (Ghosh & Abramowicz 1997; Livio et al. 1999; Cao 2003), namely the BZ and BP mechanisms. Our calculation mainly follows their method.

3.1. The BP Model

The jet power of the maximum BP model can be calculated by the following formula:

$$P_{\rm BP}^{\rm max} = 4\pi \int \frac{B_{\rm pd}^2}{4\pi} R^2 \Omega(R) dR, \tag{3}$$

where $B_{\rm pd}$ is the strength of a large-scale ordered field on the surface of a disk. Livio et al. (1999) showed that the large-scale magnetic field threading the disk and the magnetic field

Table 1
The Sample of Fermi Blazars

Name (1)	R.A. (2)	Decl. (3)	Type (4)	Redshift (5)	$\log M_{\rm BH}$ (6)	$L_{\rm disk}$ (7)	$\log L_\gamma$ (8)	$\log L_{\rm radio}$ (9)	B 10	δ (11)	$\log P_{\rm rad}$ (12)	$\log P_{\rm e}$ (13)	$\log P_{\rm B}$ (14)	$\log P_{\rm p}$ (15)	$\log L_{\rm sy}$ (16)	$\log \nu_{\rm syn}$ (17)
J0003.2+2207	0.8058	22.1302	BLL	0.1	8.1	42.74	43.71	39.96	0.0104	6.82	44.48	45.54	43.92	47.26	43.23	15.15
J0004.4-4737	1.1091	−47.6233	FSRQ	0.88	8.28	45.1	47.16	44.53	0.55	37.03	43.48	44.82	45.72	46.22	46.61	13.01
J0006.3-0620	1.5992	−6.3493	BLL	0.347	8.92	44.52	45.01	43.62	4.85	2.53	45.73	45.29	46.72	46.89	45.74	12.92
J0010.6+2043	2.6502	20.7332	FSRQ	0.598	7.86	45.34	45.94	43.19	0.0011	1.12	46.66	47.65	38.98	47.9	45.47	12.42
J0016.2-0016	4.061	−0.2806	FSRQ	1.577	8.52	45.77	48.73	45.61	0.34	21.5	44.09	42.49	45.71	41.82	47.22	12.44
J0019.6+7327	4.9031	73.456	FSRQ	1.781	9.31	46.62	49.32	45.99	0.037	39.99	45.26	46.22	43.99	45.89	47.77	12.29
J0022.0+0006	5.5154	0.1134	BLL	0.306	8.02	43.79	44.9	40.79	0.121	22.32	47.29	44.9	44.74	45.73	44.57	16.67
J0023.7+4457	5.9477	44.951	FSRQ	1.062	7.71	45.09	47.49	44.02	0.0071	142.42	42.13	46.87	42.46	47.34	46.56	12.8
J0024.7+0349	6.1975	3.8321	FSRQ	0.546	7.11	44.62	45.91	42.21	0.134	25.58	42.86	42.57	46.7	43.24	45.15	13.47
J0032.4-2849	8.1076	−28.8224	BLL	0.324	8.47	44.02	45.16	42.44	0.357	30.84	44.53	42.38	47.02	42.33	44.95	13.78
J0038.2-2459	9.5652	−24.9899	FSRQ	0.498	8.14	44.97	45.92	43.36	0.234	14.15	43.82	44.18	46.4	45.23	45.59	12.43
J0039.0-0946	9.7556	−9.7828	FSRQ	2.106	8.5	45.73	49.19	45.47	0.188	40.34	42.96	44.39	46.69	46.11	47.59	12.53
J0042.2+2319	10.5581	23.3271	FSRQ	1.425	8.73	45.49	48.02	45.52	0.149	26.59	44.08	44.59	45.29	44.69	46.92	12.27
J0043.8+3425	10.9717	34.4316	FSRQ	0.969	7.83	44.76	47.81	43.68	0.0139	69.65	43.57	46.75	41.62	46.02	45.89	13.77
J0044.2-8424	11.0711	−84.4016	FSRQ	1.032	8.52	45.87	47.3	44.54	8.17	126.7	42.5	41.89	49.16	43.5	46.58	12.96
J0045.1-3706	11.2936	−37.1065	FSRQ	1.015	8.61	45.86	47.51	44.31	0.073	23.77	43.8	45.85	44.92	47.3	46.73	12.39
J0045.7+1217	11.4309	12.292	BLL	0.255	8.82	44.18	45.49	41.98	0.134	26.45	42.47	42.89	45.69	42.93	44.78	15.56
J0047.9+2233	11.9981	22.5632	FSRQ	1.163	8.07	45.57	47.8	43.95	0.087	26	43.65	43.78	45.67	43.39	46.24	12.8
J0049.6-4500	12.4188	−45.0086	FSRQ	0.121	8.08	43.51	44.03	41.52	0.46	39.4	45.43	43.57	47.23	43.98	44.39	12.55
J0050.0-5736	12.5197	−57.6164	FSRQ	1.797	9.06	46.88	48.77	46.24	3.049	22.97	44.63	43.68	48.21	44.66	48	12.3
J0051.1-0648	12.7824	−6.8096	FSRQ	1.975	9.31	47.11	49.12	46.08	0.0375	27.51	44.71	46.9	45.1	47.8	48.23	12.48
J0056.3-0935	14.0874	−9.5997	BLL	0.103	8.96	43.22	44.39	41.36	0.096	35.19	47.28	47.2	44.81	47.41	43.92	15.78
J0058.0-0539	14.5108	−5.655	FSRQ	1.246	8.7	46.28	47.86	45.03	0.259	22.41	44.02	44.64	46.74	45.79	46.81	12.56
J0059.2+0006	14.8073	0.1166	FSRQ	0.719	8.56	46.08	46.34	44.63	0.213	27.23	43.95	44.14	46.67	43.77	46.12	13.17
J0059.3-0152	14.8361	−1.8725	BLL	0.144	8.63	43.52	44.23	40.63	0.245	52.13	45.52	43.53	44.86	42.34	44.15	16.67
J0102.8+5824	15.701	58.4092	FSRQ	0.644	9.01	46.04	47.44	44.02	0.153	27.03	45.54	45.52	45.95	45.71	46.57	12.86
J0104.8-2416	16.2146	−24.2808	FSRQ	1.747	8.98	46.05	48.77	45.22	0.193	14.89	46.17	44.9	45.41	44.32	47.83	12.2
J0105.1+3929	16.2913	39.4963	BLL	0.44	8.17	44.34	46.01	42.55	0.00948	82.07	42.47	46.33	41.37	45.95	45.76	13.45

Note. Column (1) is the 4FGL name of sources; column (2) is the R.A. in decimal degrees; column (3) is decl. in decimal degrees; column (4) is the class of the sources; column (5) is the redshift; column (6) is the black hole mass; column (7) is the accretion disk luminosity (ergs per second); column (8) is the gamma-ray luminosity (ergs per second); column (9) is the 1.4 GHz radio luminosity (ergs per second); column (10) is the magnetic field (gauss); column (11) is the Doppler factor; column (12) is the radiation jet power (ergs per second); column (13) is the electron jet power (ergs per second); column (14) is the magnetic field jet power (ergs per second); column (15) is the proton jet power (ergs per second); column (16) is the synchrotron-peak frequency luminosity (ergs per second); column (17) is the synchrotron-peak frequency.

(This table is available in its entirety in machine-readable form.)

generated by the dynamo processes are approximately

$$B_{\rm pd} \sim \frac{H}{R} B_{\rm dynamo}. \quad (4)$$

The scale height of the disk (H/R) is estimated as follows (Laor & Netzer 1989):

$$\frac{H}{R} = 15.0\dot{m}r^{-1}c_2, \quad (5)$$

where the coefficient c_2 is defined by Novikov & Thorne (1973), and other parameters are defined by

$$r = \frac{R}{R_{\rm G}},\ R_{\rm G} = \frac{GM_{\rm bh}}{c^2},\ \dot{m} = \frac{\dot{M}}{\dot{M}_{\rm Edd}},$$
$$\dot{M}_{\rm Edd} = \frac{L_{\rm Edd}}{\eta_{\rm eff}c^2} = 1.39 \times 10^{15}\ {\rm m\ kg\ s^{-1}},\ m = \frac{M_{\rm bh}}{M_\odot}, \quad (6)$$

where $\eta_{\rm eff} = 0.1$ is adopted.

Cao (2003) gave the expression of the magnetic field produced by dynamo processes in the disk as

$$B_{\rm dynamo} = 3.56 \times 10^8 r^{-3/4} m^{-1/2} A^{-1} B E^{1/2} G. \quad (7)$$

Novikov & Thorne (1973) defined the general relativistic correction factors A, B, and E. They are estimated by the following formula:

$$A = 1 + a^2x^{-4} + 2a^2x^{-6},$$
$$B = 1 + ax^{-3},$$
$$E = 1 + 4a^2x^{-4} - 4a^2x^{-6} + 3a^4x^{-8},$$
$$x = \sqrt{r}. \quad (8)$$

The Kepler angular velocity for standard accretion disk models is

$$\Omega(r) = \frac{2.03 \times 10^5}{m(a + r^{3/2})} {\rm s}^{-1}, \quad (9)$$

where a is the spin of the black hole (Cao 2003).

According to Equations (3)–(9) the maximal jet power of the BP model can be obtained if some parameters (m, $\dot{m}$, a) are specified.

3.2. The BZ Model

Livio et al. (1999) suggested that the jet power of the BZ mechanism is determined by the hole mass (m), the spin of the black hole (a), and the strength of the poloidal field threading the horizon of the black hole. The maximum jet power of the BZ model can be estimated by the following formula (e.g., MacDonald & Thorne 1982; Ghosh & Abramowicz 1997):

$$P_{\rm BZ}^{\rm max} = \frac{1}{32}\omega_F^2 B_\perp^2 R_{\rm H}^2 c a^2, \quad (10)$$

where $R_{\rm H}$ is the the horizon radius, $R_{\rm H} = [1 + (1 - a^2)^{1/2}]\ GM_{\rm bh}/c^2$. We use $\omega_F = 1/2$, $B_\perp \simeq B_{\rm pd}(R_{\rm ms})$ (e.g., MacDonald & Thorne 1982; Livio et al. 1999; Cao 2003) to estimate the maximum jet power of the BZ model. The $R_{\rm ms}$ is defined by the following formula:

$$R_{\rm ms} = R_{\rm G}\{3 + Z_2 - [(3 - Z_1)(3 + Z_1 + 2Z_2)]^{1/2}\},$$
$$Z_1 \equiv 1 + (1 - a^2)^{1/3}[(1 + a)^{1/3} + (1 - a)^{1/3}],$$
$$Z_2 \equiv (3a^2 + Z_1^2)^{1/2}. \quad (11)$$

We use Equations (4), (7) and (10) to calculate the maximal jet power of the BZ model. The scale height of the disk is proportional to the dimensionless accretion rate $\dot{m}$. Thus, the maximal jet power extracted from the disk or the spinning black hole depends on the accretion rate $\dot{m}$. In this work, the accretion rate $\dot{m}$ is adopted as a free parameter to compare our calculations with observations. The spin of black hole $a = 0.95$ is adopted (Cao 2002a, 2003).

4. Results and Discussion

The distribution of the physical parameters of the jets of Fermi blazars is shown in Figure 2. The red-shaded areas are FSRQs, and the green-shaded areas are BL Lacs. We study the difference in the physical parameter distribution of jets by using a parametric T test, a nonparametric Kruskal–Wallis H test, and a nonparametric Kolmogorov–Smirnov (K-S) test. The parameter T test is mainly used to test whether there is a difference in the average value of two independent samples. The nonparametric Kruskal–Wallis H test and the nonparametric K-S test are mainly used to test whether there are differences in the distribution of physical parameters between two independent samples. We assume that there are differences in the distribution of two independent samples among three tests simultaneously.

4.1. The Doppler Factor

The average Doppler factors of FSRQs and BL Lacs are $\langle \log \delta_{\rm FSRQs} \rangle = 1.43$ and $\langle \log \delta_{\rm BL\ Lacs} \rangle = 1.45$, respectively. According to the T test ($P = 0.45$, significant probability $P < 0.05$), K-S test ($P = 0.04$, significant probability $P < 0.05$), and Kruskal–Wallis H test ($P = 0.51$, significant probability $P < 0.05$), we find that the distribution of the Doppler factor between FSRQs and BL Lacs is not significantly different. Weaver et al. (2022) found a higher probability for FSRQs to have a larger Doppler factor than BL Lacs by using the Very Long Baseline Array (VLBA) at 43 GHz. Liodakis et al. (2018) also found that the FSRQs ($\delta_{\rm var} = 11$) have a slightly higher Doppler factor than BL Lacs ($\delta_{\rm var} = 10$) using 1029 sources observed by the Owens Valley Radio Observatory's 40 m telescope. However, we find that the FSRQs have a slightly lower Doppler factor than BL Lacs. Lister et al. (2019) studied the parsec-scale jet kinematics of 409 bright radio-loud blazars based on the VLBA at 15 GHz. Lister et al. (2019) found that the AGNs with low synchrotron-peak frequencies have the highest jet speeds (namely a high Doppler factor). Figure 3 shows the relation between the Doppler factor and synchrotron-peak frequency for Fermi blazars. We find that the AGNs with high synchrotron-peak frequencies tend to have a high Doppler factor. Our results are slightly contradictory to the results of Lister et al. (2019). There is a possible explanation that the contradiction between our results and previous studies is because there are different methods for calculating Doppler factors. Liodakis & Pavlidou (2015) also found that the Doppler factors obtained by different methods were different.

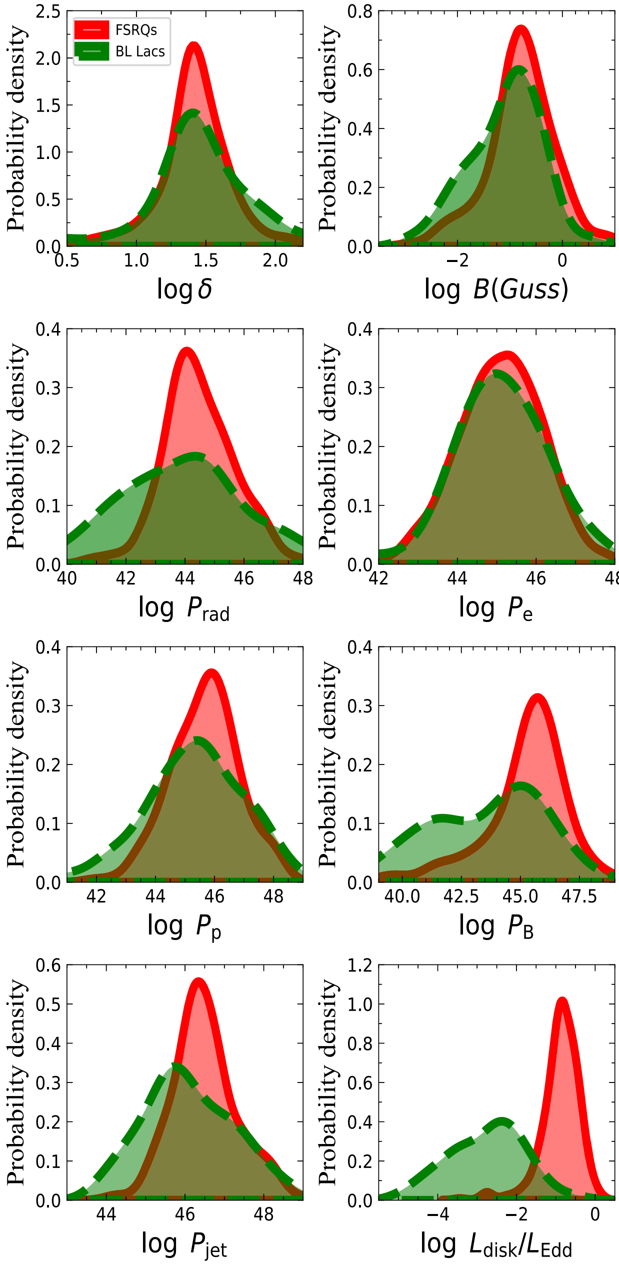

Figure 2. The distribution of physical parameters. The jet kinetic power is $P_{\rm jet} = P_{\rm B} + P_{\rm e} + P_{\rm p}$. The red line is FSRQs and the green line is BL Lacs.

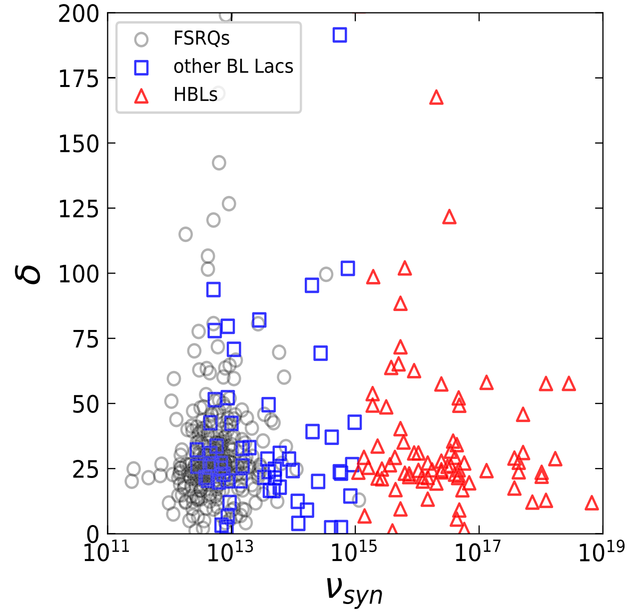

Figure 3. The Doppler factor vs. synchrotron-peak frequency for Fermi blazars. The gray circles show FSRQs; the blue squares show other BL Lacs; the red triangles show HBLs.

Weaver et al. (2022) also found that the distributions of the Doppler factor between FSRQs and BL Lacs are not significantly different based on the K-S test ($P = 0.333$). Our results are consistent with the results of Weaver et al. (2022). According to the broadband SEDs, Chen (2018) found that the mean values of the Doppler factor for FSRQs and BL Lacs are 13.87 and 27.33, respectively. The BL Lacs have a higher average Doppler factor than FSRQs. Our results are consistent with the results of Chen (2018).

4.2. The Magnetic Field

The average values of the magnetic field of FSRQs and BL Lacs are $\langle \log B_{\rm FSRQs} \rangle = -0.79$ and $\langle \log B_{\rm BL\ Lacs} \rangle = -1.09$, respectively. There is a significant difference in the average magnetic field between FSRQs and BL Lacs using the T test ($P = 7.97 \times 10^{-6}$). Through a K-S test ($P = 0.002$) and a Kruskal–Wallis H test ($P = 3.38 \times 10^{-5}$), we also find that the distributions of magnetic field between FSRQs and BL Lacs are significantly different. The FSRQs have a higher average magnetic field than the BL Lacs. Ghisellini et al. (2010) also found that FSRQs have a stronger magnetic field than BL Lacs by using 89 Fermi blazars. This is also in agreement with findings from radio VLBA observations (Pushkarev et al. 2012).

4.3. The Jet Power

The average values of the jet power of radiation from FSRQs and BL Lacs are $\langle \log P_{\rm rad,\ FSRQs} \rangle = 44.48$ and $\langle \log P_{\rm rad,\ BL\ Lacs} \rangle = 43.94$, respectively. The average values of the jet power of radiation between FSRQs and BL Lacs are significantly different using the parameter T test ($P = 0.0005$). According to the K-S test ($P = 9.18 \times 10^{-7}$) and the Kruskal–Wallis H test ($P = 0.002$), the distribution of the jet power of radiation between FSRQs and BL Lacs is significantly different. The FSRQs have a higher average jet power of radiation than the BL Lacs. Our results are consistent with the result of Foschini et al. (2015).

The average values of the jet power of electrons from FSRQs and BL Lacs are $\langle \log P_{\rm e,\ FSRQs} \rangle = 45.09$ and $\langle \log P_{\rm e,\ BL\ Lacs} \rangle = 45.07$, respectively. According to the T test ($P = 0.87$), the K-S test ($P = 0.96$), and the Kruskal–Wallis H test ($P = 0.96$), we find that the distribution of the jet power of electrons between FSRQs and BL Lacs is not significantly different.

The average values of the jet power of protons from FSRQs and BL Lacs are $\langle \log P_{\rm p,\ FSRQs} \rangle = 45.68$ and $\langle \log P_{\rm p,\ BL\ Lacs} \rangle = 45.31$, respectively. There is a significant difference in the average jet power of protons between FSRQs and BL Lacs using the T test ($P = 0.006$). Through a K-S test ($P = 0.01$) and a Kruskal–Wallis H Test ($P = 0.02$), we also find that there is a significant difference in the distribution of the jet power of protons between FSRQs and BL Lacs.

The average values of the jet power of the magnetic fields of FSRQs and BL Lacs are $\langle \log P_{\rm B,\ FSRQs} \rangle = 45.25$ and $\langle \log P_{\rm B,\ BL\ Lacs} \rangle = 43.59$, respectively. The average values of the jet power of the magnetic field between FSRQs and BL Lacs are significantly different based on the T test ($P = 2.92 \times 10^{-16}$). Through a K-S test ($P = 1.07 \times 10^{-11}$) and a Kruskal–Wallis H test ($P = 1.56 \times 10^{-13}$), the distribution of the jet power of the magnetic field between FSRQs and BL Lacs is significantly different.

The average values of jet kinetic power of FSRQs and BL Lacs are $\langle \log P_{\rm jet,\ FSRQs} \rangle = 46.52$ and $\langle \log P_{\rm jet,\ BL\ Lacs} \rangle = 46.09$, respectively. There is a significant difference in the average jet kinetic power between FSRQs and BL Lacs using the T test ($P = 1.22 \times 10^{-5}$). Through a K-S test ($P = 2.45 \times 10^{-8}$) and a Kruskal–Wallis H test ($P = 2.42 \times 10^{-5}$), we also find that there is a significant difference in the distribution of jet kinetic power between FSRQs and BL Lacs. The average values of the jet kinetic power of FSRQs are larger than that of BL Lacs (Foschini et al. 2015).

The average values of accretion disk luminosity of FSRQs and BL Lacs, in Eddington units, are $\langle \log L_{\rm disk}/L_{\rm Edd} \rangle_{\rm FSRQs} = -0.88$ and $\langle \log L_{\rm disk}/L_{\rm Edd} \rangle_{\rm BL\ Lacs} = -2.75$, respectively. The T test shows that there is a significant difference between these two averages ($P = 1.81 \times 10^{-100}$). Through a K-S test ($P = 1.48 \times 10^{-75}$) and a Kruskal–Wallis H test ($P = 2.66 \times 10^{-56}$), we also find that the distributions of accretion disk luminosity in Eddington units between FSRQs and BL Lacs are significantly different. These results may imply that the accretion modes of FSRQs and BL Lacs are different (e.g., Ghisellini et al. 2010; Sbarrato et al. 2012, 2014).

Figure 4 shows the fraction of the jet kinetic power converted to radiation ($\epsilon_{\rm rad}$), carried by relativistic electrons ($\epsilon_{\rm ele}$), and transformed into magnetic field ($\epsilon_{\rm mag}$). The average values of $\epsilon_{\rm rad}$ of FSRQs and BL Lacs are $\langle \log \epsilon_{\rm rad,\ FSRQs} \rangle = -2.04$ and $\langle \log \epsilon_{\rm rad,\ BL\ Lacs} \rangle = -2.16$, respectively. The average values of $\epsilon_{\rm ele}$ of FSRQs and BL Lacs are $\langle \log \epsilon_{\rm ele,\ FSRQs} \rangle = -1.43$ and $\langle \log \epsilon_{\rm ele,\ BL\ Lacs} \rangle = -1.03$, respectively. The average values of $\epsilon_{\rm mag}$ of FSRQs and BL Lacs are $\langle \log \epsilon_{\rm mag,\ FSRQs} \rangle = -1.27$ and $\langle \log \epsilon_{\rm mag,\ BL\ Lacs} \rangle = -2.51$, respectively. From the above results, we find that most FSRQs and BL Lacs have $\log \epsilon_{\rm rad} < 0$, which implies that the jet kinetic power of these Fermi blazars is larger than that of the radiation jet power. Ghisellini et al. (2014) also found that the jet kinetic power of Fermi blazars is larger than that of the radiation jet power. Our results are consistent with theirs. At the same time, we also find that almost all of the FSRQs and BL Lacs have $\log \epsilon_{\rm mag} < 0$ and hint at a weak magnetization of the emission region, which implies that the jet kinetic power of these FSRQs and BL Lacs are not dominated by the Poynting flux (Zdziarski et al. 2015; Paliya et al. 2017).

4.4. The Jet Formation of Fermi Blazars

The relation between jet kinetic power and black hole mass for the whole sample is shown in Figure 5. We find that there is a moderately strong correlation between jet kinetic power and black hole mass for the whole sample ($r = 0.10$, $P = 0.03$). We also use correlation analysis for every single type of sample. There is a weak correlation between jet kinetic power and black hole mass for BL Lacs ($r = 0.07$, $P = 0.38$). There is a moderately strong correlation between jet kinetic power and black hole mass for FSRQs ($r = 0.13$, $P = 0.02$). Some authors also found a significant relationship between jet power and black hole mass for FSRQs (e.g., Xiong & Zhang 2014;

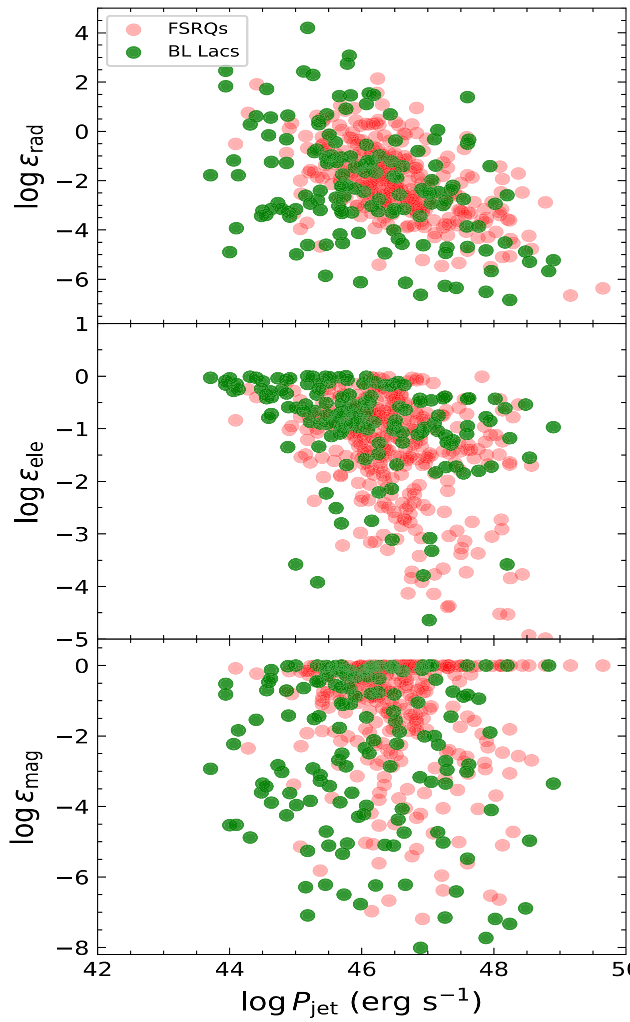

Figure 4. The fraction of the total jet power transformed into radiation (top), relativistic electrons (middle), and Poynting flux (bottom). The red dots are FSRQs and the green dots are BL Lacs.

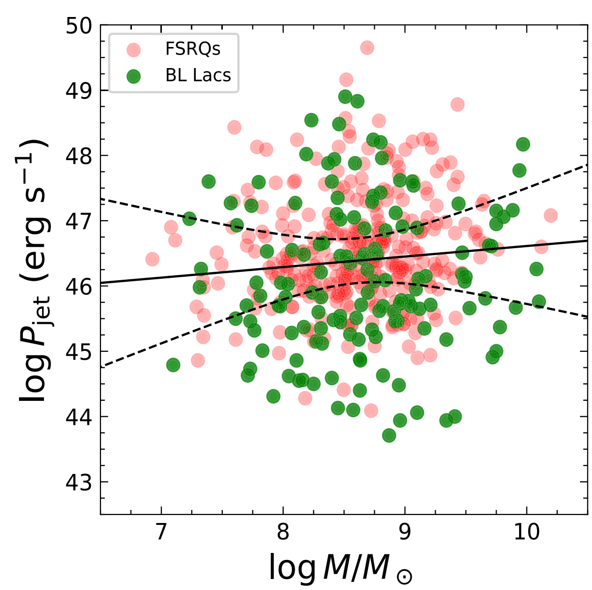

Figure 5. Relation between jet kinetic power and black hole mass. The red dots are FSRQs and the green dots are BL Lacs. The meaning of the solid and dashed lines is the same as that of Figure 4.

Zhang et al. 2014; Xiao et al. 2022). Zhang et al. (2012) also found a weak correlation between jet power and black hole mass for BL Lacs. Our results are consistent with theirs. Ghosh & Abramowicz (1997) suggested that the jet power depends on the black hole mass for an accretion disk dominated by radiation pressure. Foschini (2011) and Chen et al. (2015a) suggested that the FSRQs are in the radiation-pressure-dominated regime. However, they suggested that the jet power of the BL Lacs does not depend on the mass of the black hole, but on the accretion rate, which implies that the BL Lacs are in the gas-pressure-dominated regime (Foschini 2011; Chen et al. 2015a). These results show that FSRQs and BL Lacs have different accretion modes.

There is evidence that there is a close relationship between the jet and accretion in jetted AGNs (e.g., Rawlings & Saunders 1991; Falcke & Biermann 1995; Cao & Jiang 1999; Wang et al. 2004; Liu et al. 2006; Gu et al. 2009; Ghisellini et al. 2009, 2010, 2011; Sbarrato et al. 2012; Ghisellini et al. 2014; Sbarrato et al. 2014; Xiong & Zhang 2014; Chen et al. 2015b; Zhang et al. 2015; Paliya et al. 2017, 2019; Chen et al. 2022; Xiao et al. 2022; Zhang et al. 2022). Ghisellini et al. (2014) used the one-zone lepton model to fit the multiband data of 217 Fermi blazars to obtain the jet power. They found that there is a strong correlation between jet power and accretion disk luminosity for 217 Fermi blazars. In this work, we use a larger sample of 459 Fermi blazars to restudy the relationship between jet power and accretion disk luminosity. The jet power of 459 Fermi blazars is estimated through the one-zone leptonic model.

In the top panel of Figure 6, we show the relationship between the radiation jet power and accretion disk luminosity for all Fermi blazars (FSRQs + BL Lacs). We find a significant correlation between the radiation jet power and accretion disk luminosity for all Fermi blazars ($r = 0.22$, $P = 1.11 \times 10^{-6}$). The Spearman ($r = 0.24$, $P = 1.15 \times 10^{-7}$) and Kendall tau ($r = 0.19$, $P = 1.26 \times 10^{-8}$) tests also show a significant correlation between radiation jet power and accretion disk luminosity for all Fermi blazars. However, because the radiation jet power and accretion disk luminosity may depend on redshift, we also perform a partial correlation test. Even after excluding the general redshift dependence, we find that there is always a correlation between the radiation jet power and the accretion disk luminosity, although the significance becomes a little weak ($r_{\rm par} = 0.11$, $P = 0.02$). Paliya et al. (2017) also found that the correlation between the radiation jet power and the accretion disk luminosity becomes a little weak by using 324 Fermi blazars.

The relation between jet kinetic power and accretion disk luminosity for all Fermi blazars is shown in the bottom panel of Figure 6. We find a significant correlation between jet kinetic power and accretion disk luminosity for all Fermi blazars ($r = 0.23$, $P = 8.86 \times 10^{-7}$). The Spearman ($r = 0.24$, $P = 1.07 \times 10^{-7}$) and Kendall tau ($r = 0.17$, $P = 4.79 \times 10^{-8}$) tests also indicate a strong correlation between jet kinetic power and accretion disk luminosity for all Fermi blazars. There is still a moderately strong correlation between jet kinetic power and accretion disk luminosity when redshift is excluded ($r = 0.16$, $P = 0.0004$). Paliya et al. (2017) studied the relation between jet kinetic power and accretion disk luminosity for 324 Fermi blazars. They also found a significant correlation between jet power and accretion disk luminosity when redshift is excluded. Our results are consistent with theirs. At the same time, we also find that the jet kinetic power is slightly larger than the accretion disk luminosity for most Fermi blazars. This is not a coincidence, but the catalytic effect of the magnetic field amplified by the disk. When the magnetic energy density exceeds the energy density of the accretion material near the last stable orbit, the accretion stops and the magnetic energy decreases (Ghisellini et al. 2014). Ghisellini et al. (2014) also suggested that the jet kinetic power is larger than the accretion disk luminosity for 217 Fermi blazars.

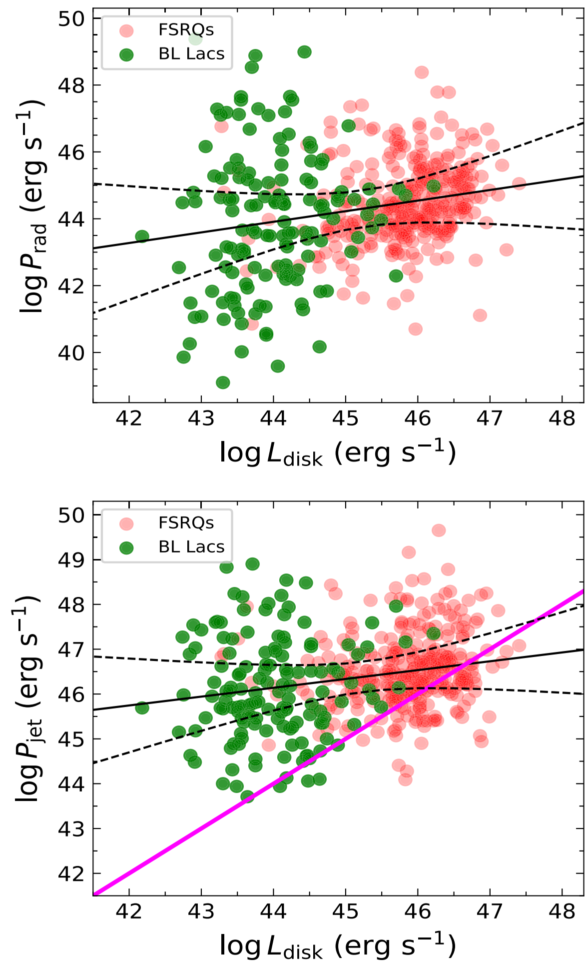

Figure 6. Relation between radiation jet power (top), jet kinetic power (bottom), and accretion disk luminosity for Fermi blazars. The red dots are FSRQs and the green dots are BL Lacs. The meaning of the solid and dashed lines is the same as in Figure 4. In the bottom plot, the pink solid line represents the one-to-one correlation. The relation between jet kinetic power, jet radiation power, and accretion disk luminosity for Fermi blazars is $\log P_{\rm rad} = (0.31 \pm 0.06)\log L_{\rm disk} + (29.95 \pm 2.91)$ and $\log P_{\rm jet} = (0.19 \pm 0.04)\log L_{\rm disk} + (37.46 \pm 1.79)$, respectively.

Figure 7 shows the relation between the ratios $L_{\rm bol}/L_{\rm Edd}$ and $P_{\rm jet}/L_{\rm bol}$. Nemmen et al. (2012) estimated the bolometric luminosity of Fermi blazars as $L_{\rm bol} = L_{\gamma} + L_{\rm sy}$ where L_{γ} is γ-ray luminosity and $L_{\rm sy}$ is synchrotron-peak frequency luminosity. Following the method of Nemmen et al. (2012), we also use the above formula to get the bolometric luminosity of Fermi blazars. The accretion rate ($\dot{m} = \dot{\rm M}/\dot{M}_{\rm Edd} \simeq L_{\rm bol}/L_{\rm Edd}$) is then estimated for our sample (Cao 2004). We use Equations (3), (4) and (7) to estimate the maximal jet power of the BP mechanism. Similarly, we also use Equations (4), (7) and (10) to estimate the maximal jet power of the BZ

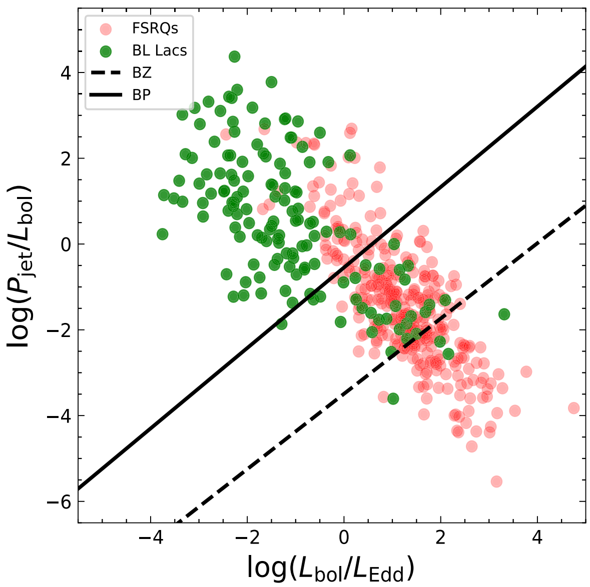

Figure 7. Relation between $L_{\rm bol}/L_{\rm Edd}$ and $P_{\rm jet}/L_{\rm bol}$. The red dots are FSRQs and the green dots are BL Lacs. Solid line: maximal jet power $P_{\rm BP}^{\rm max}$ extracted from a standard accretion disk (the Blandford–Payne mechanism). Dashed line: maximal jet power $P_{\rm BZ}^{\rm max}$ extracted from a rapidly spinning black hole $a = 0.95$ (the Blandford–Znajek mechanism).

mechanism. Because the power of the jet is proportional to the mass of the black hole ($P_{\rm jet} \propto m$; see Cao et al. 2021), the bolometric luminosity is also proportional to the mass of the black hole ($L_{\rm bol} \propto m$; see Wu & Cao 2008). Thus, the ratio of $P_{\rm jet}/L_{\rm bol}$ is only a function of the spin of the black hole and accretion rate ($\dot{m}$) (see details in Cao 2003). Therefore, we only use the black hole spin $a = 0.95$, and the accretion rate $\dot{m}$ is used as a parameter of free variation. We find that the jet kinetic power of about 68% for FSRQs is above the maximal jet power expected to be extracted from the BZ mechanism (Figure 7, dashed line). The jet kinetic power of about 97% for BL Lacs is above the maximal jet power expected to be extracted from the BZ mechanism. These results may indicate that the jets of the Fermi blazars cannot be fully explained by the BZ mechanism. Foschini (2011) also found that the BZ mechanism fails to completely account for the jet power of FSRQs. Chen et al. (2015a) compared the maximum jet power of the BZ mechanism with the observed jet power and found that the jet power of Fermi blazars cannot be fully explained by the BZ mechanism (see Figure 4 of Chen et al. 2015a).

When considering that the maximum jet power is expected to be extracted from a magnetized accretion disk, we find that the jet kinetic power of about 83% for FSRQs is below the maximal jet power expected to be extracted from a magnetized accretion disk (Figure 7, solid line). The jet kinetic power of about 23% for BL Lacs is below the maximal jet power expected to be extracted from a magnetized accretion disk. These results may suggest that the jets of FSRQs are mainly generated by the BP mechanism. Paliya et al. (2021) concluded that the overall physical properties of Fermi blazars are likely to be controlled by the accretion rate in Eddington units. In particular, FSRQs have high accretion rates in Eddington units. Xiao et al. (2022) proposed that the jets of FSRQs are powered mostly by the accretion disk. The jets of the remaining 27% of FSRQs may need to be explained by other jet models, such as magnetization-driven outflows. Cao (2018) suggested that the

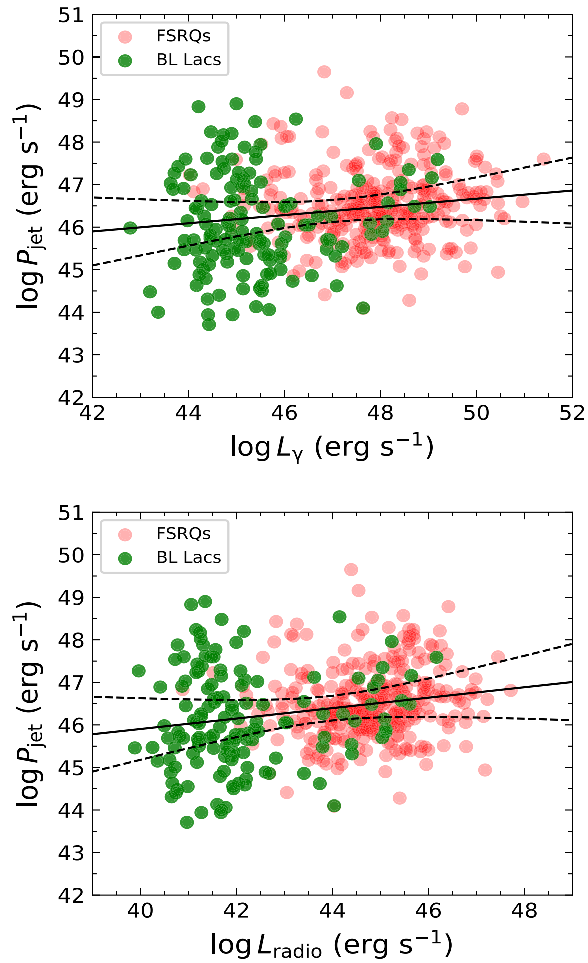

Figure 8. Relation between gamma-ray luminosity (top) and radio luminosity (bottom) and jet kinetic power for Fermi blazars. The red dots are FSRQs and the green dots are BL Lacs. The meaning of the solid and dashed lines is the same as in Figure 4.

magnetic field dragged inward by the accretion disk with magnetic outflows may accelerate the jets in blazars.

The jet kinetic power of most BL Lacs cannot be explained by both the BZ and BP mechanisms when considering the standard thin disk. Cao (2003) also found that the jet power of BL Lacs cannot be explained by both the BZ and BP mechanisms when considering the standard thin disk by using 29 BL Lacs (Figure 1 of Cao 2003). We confirm the results of Cao (2003). We find that most BL Lacs in our sample have low accretion rates. The source with advection-dominated accretion flows (ADAFs) usually has a low accretion rate (e.g., Narayan & Yi 1995). These results may imply that its accretion disk is not a standard thin disk but an ADAF. Cavaliere & D'Elia (2002) have proposed that ADAFs might be present in most BL Lacs. Cao (2002b) have suggested that most BL Lacs may have ADAFs surrounding their massive black holes.

4.5. The Jet Kinetic Power versus γ-Ray Luminosity and Radio Luminosity

Figure 8 shows jet kinetic power as a function of γ-ray luminosity (top) and 1.4 GHz radio luminosity (bottom). We find a strong correlation between jet kinetic power and γ-ray luminosity for Fermi blazars ($r = 0.17$, $P = 0.0001$). The regression result gives

$$\log P_{\rm jet} = (0.10 \pm 0.03)\log L_{\gamma} + (41.86 \pm 1.20). \quad (12)$$

There is also a strong correlation between jet kinetic power and 1.4 GHz radio luminosity for Fermi blazars ($r = 0.22$, $P = 1.77 \times 10^{-6}$). The regression result gives

$$\log P_{\rm jet} = (0.12 \pm 0.03)\log L_{\rm radio} + (40.99 \pm 1.12). \quad (13)$$

These results may imply that gamma-ray and radio emissions originated from the jet. The gamma-ray luminosity and radio luminosity can be used to indicate the jet kinetic power of Fermi blazars. Many authors have confirmed that there is a significant correlation between jet power and radio luminosity by using small samples (e.g., Willott et al. 1999; Bîrzan et al. 2008; Cavagnolo et al. 2010). Nemmen et al. (2012) also found a significant correlation between jet power and gamma-ray luminosity by using 234 Fermi blazars.

5. Conclusions

With the release of the fourth source catalog data (4FGL-DR2) of the Fermi telescope (Abdollahi et al. 2020), we can obtain high-quality quasi-simultaneous multiwavelength data of a large sample of Fermi blazars. This enables us to use a simple one-zone leptonic emission model to fit the quasi-simultaneous multiwavelength data of a larger sample of Fermi blazars and obtain some jet physical parameters, such as magnetic field, Doppler factor, jet power, and so on. At the same time, compared with the theoretical model of jets, we further discussed the jet formation mechanism of Fermi blazars. The main results are as follows:

(1) Compared with BL Lacs, FSRQs have a higher average magnetic field, radiation jet power, proton jet power, magnetic field jet power, jet kinetic power, and accretion disk luminosity in Eddington units. According to a parameter T test, nonparametric K-S test, and Kruskal–Wallis H test, we find that the distributions of these physical parameters between FSRQs and BL Lacs are significantly different. However, there is no significant difference between FSRQs and BL Lacs in the distribution of the Doppler factor and electron jet power.

(2) The Fermi blazars have $\log \epsilon_{\rm rad} < 0$, which implies that the jet kinetic power of these Fermi blazars is larger than that of the radiation jet power. At the same time, we also find that almost all of the FSRQs and BL Lacs have $\log \epsilon_{\rm mag} < 0$, which implies that the jet kinetic power of these FSRQs and BL Lacs are not dominated by the Poynting flux.

(3) There is a weak correlation between jet kinetic power and black hole mass for Fermi blazars. However, there is a moderately strong correlation between jet kinetic power and black hole mass for FSRQs.

(4) Even if the redshift is excluded, there has always been a strong correlation between jet power and accretion disk luminosity for Fermi blazars, indicating a close relationship between jets and accretion.

(5) We find that the jet kinetic power of about 82% of FSRQs is below the maximal jet power expected to be extracted from a magnetized accretion disk. This result may imply that the jets of FSRQs are mainly generated by the BP mechanism. However, the jets of BL Lacs cannot be explained by both the BZ and BP mechanisms in the case of a standard thin disk. At the same time, BL Lacs have low accretion rates. These results may imply that BL Lacs have ADAFs surrounding their massive black holes.

(6) There is a significant correlation between jet kinetic power and gamma-ray luminosity and 1.4 GHz radio luminosity for Fermi blazars. This result suggests that the jets dominate the gamma-ray and radio emissions. The gamma-ray luminosity and radio luminosity can be used to indicate the jet kinetic power of Fermi blazars.

Acknowledgments

We are very grateful to the referee for the very helpful comments and suggestions. The work is supported by the National Natural Science Foundation of China (No. 12203028, 11733002, 12121003, 12192220, 12192222, and U2031201). This work was supported by the research project of Qujing Normal University (2105098001/094). This work is supported by the youth project of the Yunnan Provincial Science and Technology Department (202101AU070146, 2103010006). Yongyun Chen is grateful for funding from the training program for talents in Xingdian, Yunnan Province. We also acknowledge the science research grants from the China Manned Space Project with No. CMS-CSST-2021-A05. Thanks to Cao Xinwu for his suggestions and opinions.

ORCID iDs

Yongyun Chen (陈永云) https://orcid.org/0000-0001-5895-0189
Junhui Fan (樊军辉) https://orcid.org/0000-0002-5929-0968
Nan Ding (丁楠) https://orcid.org/0000-0003-1028-8733
Dingrong Xiong (熊定荣) https://orcid.org/0000-0002-6809-9575

References

Abdo, A. A., Ackermann, M., Ajello, M., et al. 2009, ApJS, 183, 46
Abdo, A. A., Ackermann, M., Agudo, I., et al. 2010b, ApJ, 716, 30
Abdo, A. A., Ackermann, M., Ajello, M., et al. 2010a, ApJS, 188, 405
Abdollahi, S., Acero, F., Ackermann, M., et al. 2020, ApJS, 247, 33
Acero, F., Ackermann, M., Ajello, M., et al. 2015, ApJS, 218, 23
Ajello, M., Baldini, L., Ballet, J., et al. 2022, ApJS, 263, 24
Bîrzan, L., McNamara, B. R., Nulsen, P. E. J., Carilli, C. L., & Wise, M. W. 2008, ApJ, 686, 859
Blandford, R. D., & Payne, D. G. 1982, MNRAS, 199, 883
Blandford, R. D., & Rees, M. J. 1978, in Pittsburgh Conf. on BL Lac Objects, ed. A. M. Wolfe (Pittsburgh, PA: Univ. Pittsburgh), 328
Blandford, R. D., & Znajek, R. L. 1977, MNRAS, 179, 433
Cao, X. 2002a, MNRAS, 332, 999
Cao, X. 2002b, ApJL, 570, L13
Cao, X. 2003, ApJ, 599, 147
Cao, X. 2004, ApJ, 613, 716
Cao, X. 2018, MNRAS, 473, 4268
Cao, X., & Jiang, D. R. 1999, MNRAS, 307, 802
Cao, X., You, B., & Yan, Z. 2021, A&A, 654, A81
Cavagnolo, K. W., McNamara, B. R., Nulsen, P. E. J., et al. 2010, ApJ, 720, 1066
Cavaliere, A., & D'Elia, V. 2002, ApJ, 571, 226
Chai, B., Cao, X., & Gu, M. 2012, ApJ, 759, 114
Chen, L. 2018, ApJS, 235, 39
Chen, Y., Gu, Q., Fan, J., et al. 2022, RAA, 22, 095006
Chen, Y.-Y., Zhang, X., Xiong, D., & Yu, X. 2015a, AJ, 150, 8
Chen, Y. Y., Zhang, X., Zhang, H. J., & Yu, X. L. 2015b, MNRAS, 451, 4193
Falcke, H., & Biermann, P. L. 1995, A&A, 293, 665
Foschini, L. 2011, RAA, 11, 1266
Foschini, L., Berton, M., Caccianiga, A., et al. 2015, A&A, 575, A13
Foschini, L., Lister, M. L., Antón, S., et al. 2021, Univ, 7, 372
Ghisellini, G., Tavecchio, F., Foschini, L., et al. 2010, MNRAS, 402, 497

Ghisellini, G., Tavecchio, F., Foschini, L., & Ghirlanda, G. 2011, MNRAS, 414, 2674
Ghisellini, G., Tavecchio, F., & Ghirlanda, G. 2009, MNRAS, 399, 2041
Ghisellini, G., Tavecchio, F., Maraschi, L., Celotti, A., & Sbarrato, T. 2014, Natur, 515, 376
Ghosh, P., & Abramowicz, M. A. 1997, MNRAS, 292, 887
Gu, M., Cao, X., & Jiang, D. R. 2009, MNRAS, 396, 984
Laor, A., & Netzer, H. 1989, MNRAS, 238, 897
Liodakis, I., Hovatta, T., Huppenkothen, D., et al. 2018, ApJ, 866, 137
Liodakis, I., & Pavlidou, V. 2015, MNRAS, 454, 1767
Lister, M. L., Homan, D. C., Hovatta, T., et al. 2019, ApJ, 874, 43
Liu, Y., Jiang, D. R., & Gu, M. F. 2006, ApJ, 637, 669
Livio, M., Ogilvie, G. I., & Pringle, J. E. 1999, ApJ, 512, 100
MacDonald, D., & Thorne, K. S. 1982, MNRAS, 198, 345
Maraschi, L., & Tavecchio, F. 2003, ApJ, 593, 667
Narayan, R., & Yi, I. 1995, ApJ, 452, 710
Nemmen, R. S., Georganopoulos, M., Guiriec, S., et al. 2012, Sci, 338, 1445
Nolan, P. L., Abdo, A. A., Ackermann, M., et al. 2012, ApJS, 199, 31
Novikov, I. D., & Thorne, K. S. 1973, Black Holes (Les Astres Occlus) (New York: Gordon and Breach), 343
Paliya, V. S., Domínguez, A., Ajello, M., Olmo-García, A., & Hartmann, D. 2021, ApJS, 253, 46
Paliya, V. S., Marcotulli, L., Ajello, M., et al. 2017, ApJ, 851, 33
Paliya, V. S., Parker, M. L., Jiang, J., et al. 2019, ApJ, 872, 169
Pushkarev, A. B., Hovatta, T., Kovalev, Y. Y., et al. 2012, A&A, 545, A113
Rawlings, S., & Saunders, R. 1991, Natur, 349, 138
Sbarrato, T., Ghisellini, G., Maraschi, L., & Colpi, M. 2012, MNRAS, 421, 1764
Sbarrato, T., Padovani, P., & Ghisellini, G. 2014, MNRAS, 445, 81
TramacereA. (2020) JetSeT: Numerical modeling and SED fitting tool for relativistic jets, Astrophysics Source Code Libraryascl:2009.001
Tramacere, A., Giommi, P., Perri, M., Verrecchia, F., & Tosti, G. 2009, A&A, 501, 879
Tramacere, A., Massaro, E., & Taylor, A. M. 2011, ApJ, 739, 66
Urry, C. M., & Padovani, P. 1995, PASP, 107, 803
Vermeulen, R. C., Ogle, P. M., Tran, H. D., et al. 1995, ApJL, 452, L5
Wang, J.-M., Luo, B., & Ho, L. C. 2004, ApJL, 615, L9
Weaver, Z. R., Jorstad, S. G., Marscher, A. P., et al. 2022, ApJS, 260, 12
Willott, C. J., Rawlings, S., Blundell, K. M., & Lacy, M. 1999, MNRAS, 309, 1017
Wu, Q., & Cao, X. 2008, ApJ, 687, 156
Xiao, H., Ouyang, Z., Zhang, L., et al. 2022, ApJ, 925, 40
Xiong, D. R., & Zhang, X. 2014, MNRAS, 441, 3375
Zdziarski, A. A., Sikora, M., Pjanka, P., & Tchekhovskoy, A. 2015, MNRAS, 451, 927
Zhang, J., Liang, E.-W., Zhang, S.-N., & Bai, J. M. 2012, ApJ, 752, 157
Zhang, J., Sun, X.-N., Liang, E.-W., et al. 2014, ApJ, 788, 104
Zhang, J., Xue, Z.-W., He, J.-J., Liang, E.-W., & Zhang, S.-N. 2015, ApJ, 807, 51
Zhang, L., Liu, Y., & Fan, J. 2022, ApJ, 935, 4